

DOI: 10.1002/adma.200700564

Enhanced Photoconductivity in Thin-Film Semiconductors Optically Coupled to Photonic Crystals**

By Paul G. O'Brien, Nazir P. Kherani,* Stefan Zukotynski, Geoffrey A. Ozin, Evangellos Vekris, Nicolas Tetreault, Alongkarn Chutinan, Sajeev John, Agustín Mihi, and Hernan Míguez

Photonic crystals (PCs) are a remarkable class of materials wherein the periodicity of the index of refraction can be engineered to obtain unprecedented optical properties that have no parallels in other materials.^[1–3] Some interesting optical phenomena inherent to PCs include second harmonic generation,^[4] the superprism effect,^[5] photonic bandgaps (PBGs),^[6,7] and “slow photons”.^[8,9] It is also possible to achieve light localization^[10] within PCs by introducing defects by design that disrupt the periodicity of the index of refraction, allowing the creation of localized photon modes having frequencies that lie within the PBG of the PC.^[11,12] The ability of defect modes in PCs to confine photons is expected to provide the infrastructure for optical circuits.^[2,13–16] Moreover, lossless light propagation along PBG waveguides with coupling to quantum dots or optical cavities could provide new avenues for quantum information processing.^[17,18]

Considering that an ideal crystal is a periodic structure extending to infinity in all directions, the planar surface of a PC can actually be regarded as a 2D crystal defect. Accordingly, it is interesting to note that as in the case of defects introduced into the bulk of a PC, light can also be localized at the PC surface. For instance, it has been known for quite some time that light can propagate in localized modes along the surface of a periodically layered medium, which effectively acts a 1D PC.^[19,20]

Recently, Míguez and co-workers have investigated photon surface resonant modes in thin films coupled to PCs.^[21] One structure studied in this work has been fabricated by depositing a homogeneous silica layer on top of a silica inverse colloidal crystal. The results of the study indicate that upon illumination of this layer of silica with normally incident light at certain frequencies within the bandgap of the PC, the electromagnetic field near the PC/film interface is amplified with respect to the electromagnetic fields in the surrounding regions. This phenomenon arises from partial light localization at the modified PC surface, which behaves as an optical dopant or defect.

Structures similar to those studied by Míguez and co-workers have been used to enhance the efficiency of Grätzel cells comprising dye-sensitized titania electrodes shaped as PCs. The observed improvements were initially attributed to slow photons propagating through the PC structure;^[22] however, it has subsequently been pointed out that this hypothesis does not account for all of the observed results and that the improvements arise primarily from light localization at the surface of the structure.^[23]

The objective of the research reported herein is two-fold. The first objective is to demonstrate that the photoconductivity of a semiconductor film can be amplified by optically coupling the film to a PC surface. Indeed, in this construct, the film does not itself need to be periodically structured. The second objective is to show that the photoconductivity enhancement attainable from surface resonant modes in thin films coupled to PC surfaces is greater than the enhancement that can be achieved by depositing a perfect mirror (PM) onto the backside of this film.

To address the first objective, we have compared the measured quantum efficiencies (QEs) of a thin hydrogenated amorphous silicon (a-Si:H) film deposited on a glass substrate for two different structures. One structure is the film–PC construct shown in Figure 1a, wherein an opaline^[24] PC is deposited onto the backside of a thin a-Si:H film, whereas the sec-

[*] Prof. N. P. Kherani, Prof. S. Zukotynski
The Edward S. Rogers Sr. Department of Electrical and Computer Engineering
University of Toronto
10 King's College Road, Room GB254B, Toronto, ON M5S 3G4 (Canada)
E-mail: kherani@ecf.utoronto.ca
Prof. N. P. Kherani, P. G. O'Brien
Department of Materials Science and Engineering
University of Toronto
184 College Street, Room 140, Toronto, ON M5S 3E4 (Canada)
Prof. G. A. Ozin, E. Vekris, Dr. N. Tetreault
Materials Chemistry Research Group, Department of Chemistry
University of Toronto
80 St. George Street, Toronto, ON M5S 3H6 (Canada)
Dr. A. Chutinan, Prof. S. John
Physics Department
University of Toronto
60 St. George Street, Toronto, ON M5S 1A7 (Canada)
A. Mihi, Dr. H. Míguez
Centro de Tecnología Nanofotónica, Edificio I-4
Universidad Politécnica de Valencia
Camino de Vera s/n, E-46022 Valencia (Spain)

[**] GAO and SJ are Government of Canada Research Chairs in Materials Chemistry and Physics, respectively. GAO, NPK, SZ, and SJ are deeply indebted to the Natural Sciences and Engineering Research Council of Canada and the University of Toronto for financial support of this work. HM acknowledges partial funding provided by the Ramón Areces Foundation and the Spanish Ministry of Science and Education under grant MAT2005-03 028. The authors would like to thank Dr. Davit Yeghikyan and Dr. Stefan Costea for their assistance in carrying out the hydrogenated amorphous silicon depositions and the quantum efficiency measurements.

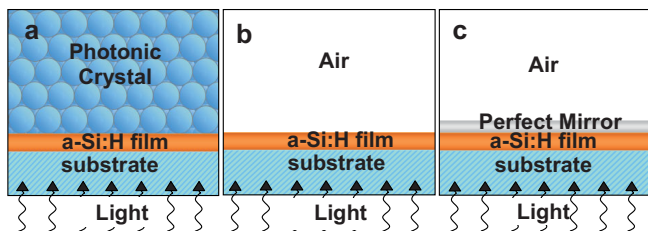


Figure 1. Schematic depiction of the structures investigated in this work. a) An opaline PC deposited onto a thin a-Si:H film (referred to as the film-PC construct). b) A bare a-Si:H film deposited onto a glass substrate. c) A PM on the backside of a thin a-Si:H film (referred to as the film-PM construct).

ond structure, as shown in Figure 1b, is a bare a-Si:H film. The QE of each of these structures has been deduced by measuring the current through the a-Si:H film with normally incident light entering from the glass side (as shown in Fig. 1) and impinging onto the film. Normalizing the QE measured for the film-PC construct to that measured for the bare film yields a QE enhancement factor, which is effectively the photoconductivity enhancement factor.

To address the second objective, we have performed finite difference time domain (FDTD)-based calculations^[25,26] to quantify and compare the photoconductivity of the film-PC construct to a hypothetical case wherein a PM is deposited onto the rear side of the film, as shown in Figure 1c. The schematic shown in Figure 1c is referred to as the film-PM construct. Before presenting the results we first discuss some relevant characteristics of the film-PC construct.

The film-PC construct comprises an opaline PC deposited onto an a-Si:H film. An opaline PC can be described as an array of glass spheres close-packed into a face-centered cubic (fcc) crystal lattice. Opaline PCs do not possess a full photonic bandgap but do exhibit a narrow stopgap ($\Delta\omega/\omega = 5.5\%$) between the second and third photonic bands in the [111] direction. The opaline PCs have been fabricated using the vertical deposition method,^[27] and in this case the [111] direction in the PC is aligned along the normal of the substrate surface on which the PC is grown. In this work, the QE has been measured using normally incident light, thus obviating the need of a PC with a complete photonic bandgap. Light scattering from the surfaces of the glass substrate and a-Si:H films is insignificant because these surfaces are smooth, exhibiting an average roughness of less than a few nanometers.

We note that the photoconductivity of a thin film can also be enhanced by replacing the opaline PC in the thin-film-PC construct with a dielectric mirror, since the only stopgap we are using is in the [111] direction.^[28] However, as discussed below, some of the normally incident photons striking the opaline PC in the film-PC construct are diffracted into surface resonant modes and propagate along the film rather than across it. These photons are subject to a longer interaction time with the semiconductor film and are more likely to be absorbed. Also, opaline PCs are easily fabricated, and can additionally be inverted with silicon to obtain a PC with a full

photonic bandgap,^[29] which may be useful for other more sophisticated light-harvesting constructs.

To investigate the effects of shifting the [111] stopgap of the PC on the photoconductivity enhancement factor, we have deposited three different opaline PCs comprising approximately 40 layers of silica spheres with different diameters ($d = 190, 274, \text{ and } 343\text{ nm}$) onto a-Si:H films of comparable thickness ($t = 250 \text{ to } 300 \text{ nm}$). The number of layers of silica spheres and the thickness of the a-Si:H films have been determined from cross-sectional scanning electron microscopy (SEM) imaging of the samples at locations where the QE is measured. To illustrate this construct, cross-sectional SEM images of an opaline PC with 38 layers of spheres ($d = 274 \text{ nm}$ diameter) deposited onto an a-Si:H film, and the corresponding $t = 254 \text{ nm}$ thick a-Si:H film (after removal of the spheres) are shown in Figure 2a and b, respectively. The measured photoconductivity enhancement factors for the

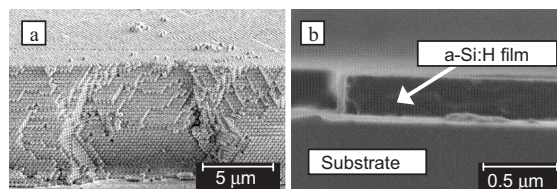


Figure 2. Cross-sectional SEM images of samples with the film-PC construct. a) SEM cross-sectional image of an opaline PC deposited onto an a-Si:H film. b) SEM cross-sectional image of a $t = 254 \text{ nm}$ thick a-Si:H layer deposited onto Corning 1737 glass.

three film-PC constructs, together with the enhancement factors calculated using a scalar wave approximation (SWA) are shown in Figures 3a-c, whereas Figure 3d shows a picture of the film-PC construct with $d = 343 \text{ nm}$ diameter sphere opals.

The measured and calculated photoconductivity (absorption) enhancement factors shown in Figure 3a are approximately unity throughout the spectral region of interest indicating that the addition of a PC comprising $d = 190 \text{ nm}$ diameter spheres does not enhance absorption in the film. This is owing to the fact that an opaline PC comprising silica spheres of this size has a directional [111] stopgap centered at $\lambda = 410 \text{ nm}$. Since a-Si:H is highly absorbing in this spectral range,^[30] the majority of the incident light is absorbed during its first pass through the film, and there is very little opportunity for further enhancement.

The photoconductivity enhancement factor measured for the film-PC sample with an opaline PC of $d = 274 \text{ nm}$ spheres with a stopgap centered at $\lambda = 591 \text{ nm}$ reaches a peak value of 1.5 at a wavelength of $\lambda = 610 \text{ nm}$ (Fig. 3b). The photoconductivity enhancement factor calculated using the SWA also peaks at $\lambda = 610 \text{ nm}$, although with a higher peak value of 3.28. We attribute this discrepancy primarily to the error in the assumed value of the extinction coefficient κ (where $\alpha = 4\pi\kappa/\lambda$ is the absorption coefficient) used to model the a-Si:H film. Owing to the onset of the absorption edge of the

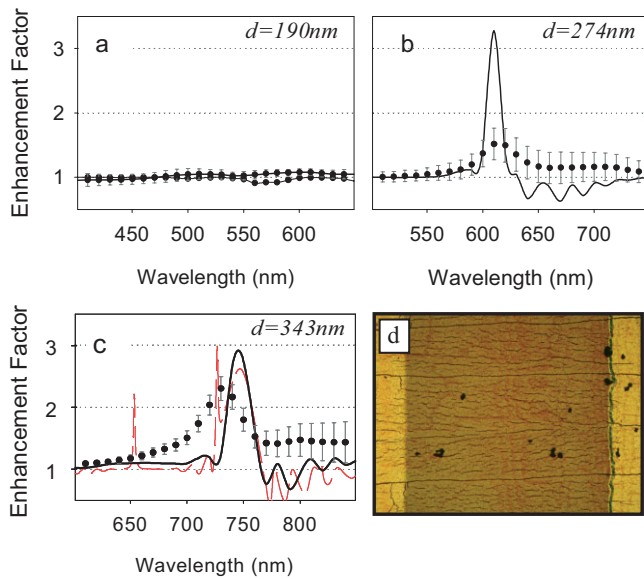


Figure 3. Influence of the stopgap position on the photoconductivity enhancement factor for three film-PC constructs using $d = 190$, 274 , and 343 nm diameter sphere opals. The [111] stopgap of the opaline PC is centered at a) $\lambda = 410$ nm, b) $\lambda = 591$ nm, and c) $\lambda = 740$ nm. In each plot, the absorption enhancement factor, calculated using the SWA method, is plotted as a solid line, whereas the experimental results are shown as solid circles with corresponding error bars. The enhancement factor calculated using the FDTD method is also shown for the $d = 343$ nm sample (dashed red line). d) A picture of the film-PC construct comprising $d = 343$ nm diameter sphere opals corresponding to the enhancements plotted in (c). The dark region represents the 1 mm gap between the aluminum contacts, which appear as brighter areas on the left and right edges of the image. Note that numerous cracks and voids can be seen in the opaline PC deposited onto the a-Si:H film.

a-Si:H films, there is a large degree of uncertainty in the value of κ for wavelengths longer than 600 nm. The assumed value of κ used in the SWA calculation is 0.2; however, when this number is doubled, the calculated photoconductivity enhancement factor decreases significantly from 3.28 to 2.23. We proceed to further discuss this point in the following paragraphs.

The measured and simulated photoconductivity enhancement factors for the $d = 343$ nm sample (Fig. 3c), wherein the opaline PC has a [111] stopgap centered at $\lambda = 740$ nm, have peak values of 2.3 and 2.74 at $\lambda = 730$ nm and $\lambda = 750$ nm, respectively. As with the previous sample, the measured peak photoconductivity enhancement factor is lower than the calculated value. However, in this case the difference between the two peak values does not arise from an erroneous value for κ but is instead attributed to the presence of cracks and vacancies within the opaline PC, which serve to broaden and weaken the photonic stopgap.^[31,32] Variations in κ are not expected to have a major impact on the simulated values of the photoconductivity enhancement factor, since the value of κ over the region of interest ($700 \text{ nm} < \lambda < 750 \text{ nm}$) is known to be small. Indeed, values reported in the literature are typically on the order of 10^{-4} .^[30] Calculations of the photoconductivity enhancement factor for κ values ranging from 2×10^{-7} to

2×10^{-2} (not shown), a difference of five orders of magnitude, reveal a peak value decrease of only 8.5 %.

From the preceding discussion it can be deduced that in the limit of weak absorption the photoconductivity enhancement factor is independent of the absorption coefficient of the thin-film material. In the opposite limit of high absorption, the majority of the light entering the film is absorbed in one pass through the film and the addition of a PC backing does not affect the amount of light absorbed. Consequently, the photoconductivity enhancement factor in this case is simply unity, indicating no enhancement. At intermediate wavelengths for which the absorption coefficient is neither significant nor negligible, the photoconductivity enhancement factor is highly dependent on κ .

We have also plotted the photoconductivity enhancement factor for the $d = 343$ nm sample using a FDTD-based calculation (dashed red line in Fig. 3c). The FDTD calculation reveals a strong resonant mode within the PBG at $\lambda = 727$ nm and a second resonant mode outside the PBG at $\lambda = 653$ nm. The mode profile for the $\lambda = 727$ nm resonant mode (Fig. 4) reveals that light propagation within these resonant modes oc-

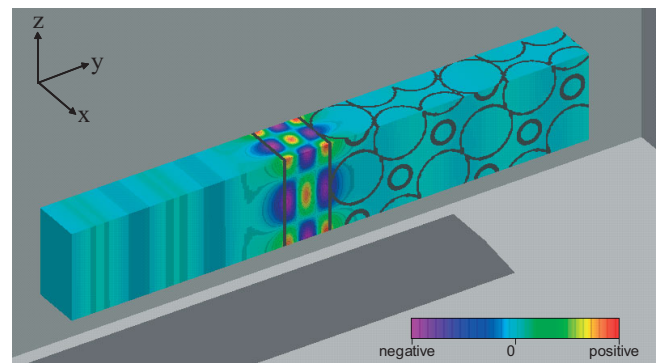


Figure 4. Profile of the $\lambda = 727$ nm surface resonant mode in the film-PC construct of Figure 3c. The figure also shows a solid rectangular cross section profiling the electric field on resonance in the film-PC construct (outlined in black). Normally incident light propagates along the y -axis which is parallel to the [111] direction of the opaline PC. The xz -plane is equivalent to the [111] plane and the lattice constants in the x - and z -directions are a and $\sqrt{3}a$, respectively. Thus, the xz planar cross section of the plotted volume corresponds to one unit cell ($a \times \sqrt{3}a$). The magnitude of the electric field is the greatest within the two straight black lines outlining the a-Si:H film.

curs in the planar direction. Thus, the PC scatters incident photons into these planar resonant modes having a wavevector in the planar direction that is determined by the periodicity of the PC surface. Cracks and other defects within the PC (Fig. 3d) tend to attenuate and widen the resonant mode, and consequently the associated photoconductivity enhancement factor is measured as a comparatively weak enhancement over a broad spectral range. The additional enhancement arising from the presence of these planar surface modes explains the blue-shifting of the measured peak enhancement factor

relative to the one calculated using the SWA. These planar surface resonant modes are not accounted for by the SWA, which only analyzes the optical properties of the structure in 1D, along the [111] direction normal to the film surface.

Although planar surface resonant modes may appear at any wavelength, resonance is strongest in modes appearing within the stopgap. We have considered two similar film-PC constructs hosting a surface resonant mode either just inside or just outside the stopgap. Upon reducing the number of layers in the PC to unity, the strengths of the resonances in both modes is comparable. However, we have performed FDTD calculations (not shown) confirming that the resonance of surface modes appearing within the stopgap is enhanced as the number of layers in the PC is increased from unity, whereas the resonance of surface modes appearing outside the stopgap is nearly independent of the number of PC layers. The absorption enhancement is maximized when the surface resonant modes appear within the [111] stopgap. The wavelength at which these in-plane resonance modes occur is highly dependant on the thickness of the semiconductor film. Accordingly, we have also studied the influence of the film thickness on the photoconductivity enhancement factor.

The measured and calculated (FDTD) photoconductivity enhancement factors obtained when an opaline PC with 40 layers of $d = 343$ nm diameter spheres is deposited onto a-Si:H films with thicknesses $t = 96$ and 110 nm are shown in Figure 5a and b, respectively.

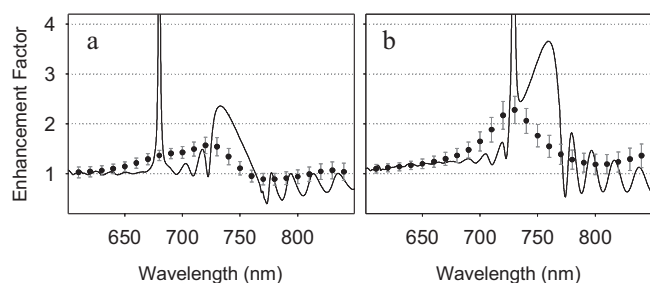


Figure 5. Effect of changing the film thickness on the photoconductivity enhancement factor. The measured (solid circles) and calculated (solid line) photoconductivity enhancement factors for film-PC constructs upon depositing an opaline PC comprising $d = 343$ nm spheres onto a) $t = 96$ nm and b) $t = 110$ nm thick a-Si:H films.

As shown in Figure 5a, the measured photoconductivity enhancement factor for the $t = 96$ nm thick a-Si:H film exhibits a peak value of 1.6. The corresponding photoconductivity enhancement factor calculated using the FDTD method exhibits a surface resonant mode outside the stopgap at $\lambda = 680$ nm. The measured photoconductivity enhancement factor for the $t = 110$ nm thick a-Si:H film (Fig. 5b) exhibits a peak value of 2.3. The greater enhancement factor achieved in the $t = 110$ nm film is partially attributed to the fact that the surface resonant mode, possessing a mode profile similar to that shown in Figure 4, exists within (rather than outside) the

[111] stopgap in the $t = 110$ nm film-PC construct. The peak value of the photoconductivity enhancement in the $t = 110$ nm film contains contributions from both the surface resonant mode as well as the PBG reflection from the [111] stopgap.

From the preceding discussion it is clear that the film thickness in the film-PC construct can be tailored so that resonant modes appear within the photonic stopgap and serve to further enhance the photoconductivity within the thin semiconductor film. We now demonstrate that the photoconductivity enhancement gained from these surface resonant modes can be greater than that attainable in a film-PM construct over a range of frequencies. The absorption spectra, calculated using the FDTD method, for both the film-PC and film-PM constructs are shown in Figure 6a. The thickness of the film is $t = 110$ nm for both cases and the opaline sphere

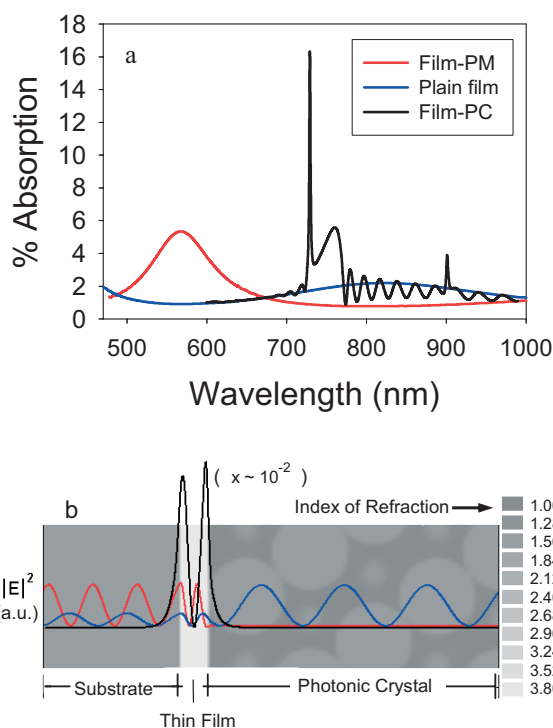


Figure 6. Absorption spectra and electric-field distributions for the film-PC and film-PM constructs. a) Absorption spectra for a film-PC construct (black line), a film-PM construct (red line), and a bare film (blue line). In each case the semiconductor film is $t = 110$ nm thick and the opaline PC in the film-PC construct comprises 40 layers of $d = 343$ nm silica spheres. The film material is assumed to have an index of refraction and extinction coefficient of $n = 3.8$ and $\kappa = 0.02$, respectively. b) A comparison of the electric field within the semiconductor film to the electric field in the surrounding regions for the film-PC, film-PM, and bare-film constructs. The relative spatial distribution of the electric-field intensity (arbitrary units) at the resonant wavelength ($\lambda = 730$ nm) in the film-PC construct (black line) and bare-film construct (blue line) is shown superimposed over a dielectric map of the film-PC structure. The electric-field distribution in the film-PM construct at its resonant wavelength ($\lambda = 567$ nm) is also shown (red line) (all plots have been simulated using the FDTD method and the plot of $|E|^2$ for the film-PC construct has been scaled down by more than two orders of magnitude).

diameter is $d = 343$ nm. The absorption spectrum of a bare $t = 110$ nm thick a-Si:H film is also shown for comparison.

The absorption spectrum of the film-PC construct exhibits a sharp peak reaching 16% at $\lambda = 730$ nm, corresponding to a surface resonant mode similar to that illustrated in Figure 4. For the film-PM construct, the maximum absorption is just under 6%, occurring at a wavelength of $\lambda = 567$ nm. The maximum absorption in the film-PC construct, other than the absorption at the resonant wavelength, is similar to that of the mirror. This suggests that the PC behaves as a PM over stopgap wavelengths with the added possibility of designing the film-PC construct such that surface resonant modes appear within the stopgap of the PC. In this case, the photoconductivity enhancement factor, with contributions from both the surface resonant mode as well as the PBG reflection, can be made to exceed that achievable in the film-PM construct.

The spatial distribution of the electric field in the film-PC construct at the resonant wavelength of $\lambda = 730$ nm and the electric-field distribution in the film-PM construct at the wavelength corresponding to the absorption maximum ($\lambda = 567$ nm) are plotted in Figure 6b. The electric-field distribution on resonance in the film-PC construct is almost 1000 times greater within the semiconductor film than in the surrounding regions as compared to no amplification of the electric field in the film-PM construct.

The ability of the film-PC and film-PM constructs to confine light can also be compared by treating these structures as optical cavities and calculating their quality (Q) factors. Here, the Q factor is defined as 2π multiplied by the number of oscillation cycles required for the energy of the electromagnetic field in the cavity to decay to $1/e$ of its initial value. The Q factor can be determined from the following relation:^[33]

$$U(t) = U(0)\exp[-(\omega_0 t)/Q] \quad (1)$$

where $U(t)$ is the total energy of the electric field in the cavity at time t , ω_0 is the resonant frequency of the cavity, and Q is the quality factor. We have determined the Q -factor associated with the resonant mode plotted in Figure 6b by calculating the time required for the electric field in the film to decay when a Gaussian pulse, centered at the resonant frequency, is injected into this cavity at the midpoint of the a-Si:H film. The results yield a Q factor of approximately 17 000 for the resonant mode in the film-PC construct as compared to about 64 for the resonant mode in the film-PM construct.

In conclusion, we have shown that the photoconductivity in a thin semiconductor film can be enhanced by depositing a PC onto the backside of this film. The greatest enhancement due to PBG reflection is obtained when the opaline PC is designed such that the [111] photonic stopgap exists over a range of frequencies for which the semiconductor is weakly absorbing. We have experimentally verified that the photoconductivity in the film can be further enhanced by designing the film thickness such that surface resonant modes appear within the [111] stopgap. Specifically, the photoconductivity of a

$t = 96$ nm thick a-Si:H film is found to increase by 60% when a 40-sphere-layered opaline PC, comprising $d = 343$ nm diameter spheres, is deposited onto the backside of the film. However, upon increasing the thickness of the film to $t = 110$ nm, surface resonant modes having wavelengths within the [111] stopgap appear in the film-PC construct, and in this case the photoconductivity is found to increase by 130%.

FDTD-based calculations have been used to compare the absorption enhancement achieved by depositing a 40-sphere-layered opaline PC onto the backside of a $t = 110$ nm thick a-Si:H film to the enhancement achieved for the theoretical case in which a PM is placed on the backside of this film. We have found that the absorption in the film-PC construct exceeds that of the film-PM construct over a narrow range of wavelengths. For the film-PC construct, the absorption at the resonant frequency reaches a peak value of 16% as compared to a peak value of 6% for the film-PM construct. Also, the Q factor associated with the film-PC resonant mode is found to be much larger than that of the resonant mode in the film-PM construct.

The semiconductor film does not need to be periodically structured to exhibit enhanced photoconductivity. This simplicity may render the film-PC construct useful in a variety of devices. For example, in resonant-cavity-enhanced photodetectors^[34] it may be desirable to increase photon absorption over only a narrow range of frequencies. This can be accomplished by optically coupling a thin film to the surface of a PC having a narrow bandgap, where the thickness of the film is tuned such that one surface resonant mode exists within the spectral region of interest and is within the PBG. In this construct, the photoconductivity within the narrow bandgap is enhanced because of contributions from both the high PBG reflection as well as the surface resonant mode. The film-PC construct may also be useful for thin-film solar cells. In this case, the range of wavelengths over which the photoconductivity is enhanced can be increased by inverting the opaline PC to obtain a larger stopgap, thereby broadening the spectral range over which high reflection is achieved. Also, the number of resonant states appearing within the stopgap can be increased by increasing the film thickness. This would be applicable to crystalline silicon solar cells wherein the thickness of the absorbing region is on the order of 100 μm as compared to film thicknesses of 100 to 300 nm for the samples studied here.

Experimental

Sample Fabrication: To fabricate the samples shown in Figure 1a and b, 1.1 mm thick Corning 1737 glass substrates were first cleaned in a 3:1 (v/v) solution of sulfuric-acid/hydrogen-peroxide and then rinsed with distilled water. Plasma enhanced chemical vapor deposition, using the dc saddle field [35,36], was used to deposit thin films of a-Si:H ranging in thickness from about 100 to 300 nm onto the glass substrates. Two square coplanar aluminum contacts (1 cm^2), spaced apart by 1 mm, were subsequently deposited via physical vapor deposition onto the a-Si:H films. Silica spheres having different diameters (190, 274, and 343 nm) were prepared using a modified Stöber method [37,38], and deposited as a close-packed fcc PC onto the a-Si:H film between the two Al contacts using a vertical assembly technique [27], thus forming the film-PC construct.

Optical Measurements: A monochromatic beam of light was obtained using a quartz halogen lamp and a CVI Spectral Products CM110 monochromator. The monochromatic beam was incident from the glass side with a spot size that was approximately 2 mm long and 0.5 mm wide. The beam was centered onto the a-Si:H film between the two Al contacts. A beam splitter was used to direct 20% of the incident light onto a photodetector (a Si-InGaAs photodiode pair) to measure the power of the incident beam in order to determine the number of incident photons. A 50 V bias was applied between the Al contacts and the current through the 1 mm gap between the two contacts was measured using a Keithley 6517 electrometer. The current was measured as the wavelength of the incident beam was increased in increments of 10 nm starting at 400 nm and ending at 900 nm. Having measured the QE of the thin a-Si:H-film-opaline-PC construct, the opaline PC on the backside of the film was removed and the QE of the bare film alone was subsequently measured. To remove the PC layer, the silica spheres were gently brushed aside using a small piece of cotton soaked in ethanol. Upon removing the spheres in this fashion the sample position was unchanged. As a result, when the QE was measured a second time (now without the PC), the incident beam struck the sample at the same spot. This procedure avoided any complications that might possibly arise due to inhomogeneities in the thickness of the a-Si:H film. It also ensured that the distance between the Al contacts and the illuminated region of the sample was the same both with and without the PC layer. The QE measured with the opaline PC present was normalized to the QE measured for the bare a-Si:H film to determine the photoconductivity enhancement factor.

Modeling: Assuming that the photoconductivity of a semiconductor film at a given wavelength, λ_i , is directly proportional to the number of absorbed photons of wavelength λ_i , we modeled the photoconductivity enhancement in the film-PC construct by calculating an absorption enhancement factor. This factor is defined as the absorption of the a-Si:H film with a PC on the backside normalized against the absorption of the same film without a PC. The absorption enhancement factor was calculated using both 1D SWA and exact 3D FDTD methods. The SWA provides a good description of the reflection and transmission spectra in highly symmetric directions for the lower level photonic bands in a PC [23]. The SWA consists of replacing the 3D PC with a 1D Bragg stack exhibiting the same stopgap between the second and third bands in the [111] direction. FDTD methods were used to perform a full vectorial analysis of the structure and to model the in-plane resonant modes that were not detected by the SWA-based calculations. For film-PC samples where the opal diameter is 343 nm, the PBG is centered at $\lambda = 740$ nm. In this spectral region, the dependence of the photoconductivity enhancement factor on κ is negligible. For film-PC samples in which $d = 343$ nm, the photoconductivity enhancement factor was calculated using the FDTD method (Figs. 3c, 4a, and 4b). The FDTD method was also used to determine the strength of the resonant modes in the film-PC and film-PM constructs. As depicted in Figure 1, the light was incident from the normal direction. In the normal direction, the ends of the structures were truncated with a perfectly matched layer [25]. Periodic boundary conditions were used in the transverse direction. The mesh size was kept less than $\lambda/20$ in all cases. The convergence of the FDTD method was verified by reducing the mesh spacing to $\lambda/30$. The SWA- and FDTD-based calculations require knowledge of the index of refraction (n) and the extinction coefficient (κ) of the film material. To determine n and κ for our a-Si:H films, a modified Levenberg-Marquardt algorithm was employed to iteratively calculate the reflection and transmission spectra of the thin a-Si:H film as the values of n and κ were varied. The assumed n and κ values were those that provided the best fit (SCI Software's Film Wizard was used to fit the data) between the calculated reflection and transmission and the reflection and transmission measured using a spectrometer (SD2000, Ocean Optics).

Received: March 6, 2007

Revised: August 22, 2007

Published online: November 12, 2007

- [1] C. Lopez, *Adv. Mater.* **2003**, *20*, 1679.
- [2] L. Thylen, M. Qui, S. Anand, *ChemPhysChem* **2004**, *5*, 1268.
- [3] J. D. Joannopoulos, *Nature* **1997**, *386*, 143.
- [4] A. Fedyanin, O. Aktsipetrov, D. Kurdyukov, *Appl. Phys. Lett.* **2005**, *87*, 151 111.
- [5] T. Ochiai, J. Sanchez-Dehesa, *Phys. Rev. B: Condens. Matter* **2001**, *64*, 245 113.
- [6] S. John, *Phys. Rev. Lett.* **1987**, *58*, 2486.
- [7] E. Yablonovitch, *Phys. Rev. Lett.* **1987**, *58*, 2059.
- [8] A. Imhof, W. L. Vos, R. Sprik, A. Lagendijk, *Phys. Rev. Lett.* **1999**, *83*, 2942.
- [9] J. I. L. Chen, G. von Freymann, S. Y. Choi, V. Kitaev, G. A. Ozin, *Adv. Mater.* **2006**, *18*, 1915.
- [10] S. John, *Phys. Rev. Lett.* **1984**, *53*, 2169.
- [11] S. John, *Phys. Today* **1991**, *44*, 32.
- [12] E. Yablonovitch, T. J. Gmitter, *Phys. Rev. Lett.* **1991**, *67*, 3380.
- [13] A. Arsenault, S. Fournier-Bidoz, B. Hatton, H. Míguez, N. Tetreault, E. Vekris, S. Wong, S. M. Yang, V. Kitaev, G. A. Ozin, *J. Mater. Chem.* **2004**, *14*, 781.
- [14] A. Chutinan, S. John, *Phys. Rev. Lett.* **2003**, *90*, 123 901.
- [15] A. Chutinan, S. John, *Opt. Express* **2006**, *14*, 1266.
- [16] E. Vekris, V. Kitaev, G. von Freymann, D. Perovic, J. Aitchison, G. A. Ozin, *Adv. Mater.* **2005**, *17*, 1269.
- [17] J. Vukovic, D. England, D. Fattal, E. Waks, Y. Yamamoto, *Physica E* **2006**, *32*, 466.
- [18] Q. Minghao, E. Lidorikis, P. T. Rakich, S. Johnson, J. D. Joannopoulos, E. P. Ippen, H. L. Smith, *Nature* **2004**, *429*, 538.
- [19] P. Yeh, A. Yariv, A. Y. Cho, *Appl. Phys. Lett.* **1978**, *32*, 104.
- [20] W. Ng, P. Yeh, P. C. Chen, A. Yariv, *Appl. Phys. Lett.* **1978**, *32*, 370.
- [21] A. Mihi, H. Míguez, S. Rubio, I. Rodríguez, F. Meseguer, *Phys. Rev. B: Condens. Matter* **2005**, *71*, 125 131.
- [22] S. Nishimura, N. Abrams, B. A. Lewis, L. I. Halaoui, T. E. Mallouk, K. D. Benkstein, J. van de Lagemaat, A. J. Frank, *J. Am. Chem. Soc.* **2003**, *125*, 6303.
- [23] A. Mihi, H. Míguez, *J. Phys. Chem. B* **2005**, *109*, 15 968.
- [24] D. Norris, E. G. Arlinghaus, L. Meng, R. Heiny, L. E. Scriven, *Adv. Mater.* **2004**, *16*, 1393.
- [25] A. Taflove, S. C. Hagness, *Computational Electrodynamics: The Finite-Difference Time-Domain Method*, 3rd ed., Artech House, Norwood, MA **2005**.
- [26] *Electromagnetic Theory and Applications for Photonic Crystals* (Ed: H. Yasumoto), Taylor and Francis, Boca Raton, FL **2006**.
- [27] P. Jiang, J. F. Bertone, K. S. Hwang, V. Colvin, *Chem. Mater.* **1999**, *11*, 2132.
- [28] A. Chin, T. Y. Chang, *J. Vac. Sci. Technol. B* **1990**, *8*, 339.
- [29] A. Blanco, E. Chomski, S. Grabtchak, M. Ibisate, S. John, S. W. Leonard, C. Lopez, F. Meseguer, H. Míguez, J. P. Mondia, G. A. Ozin, O. Toader, H. M. van Driel, **2000**, *405*, 437.
- [30] *Handbook of Optical Constants* (Ed: E. D. Palik), Academic, Boston, MA **1991**.
- [31] S. L. Kuai, Y. Z. Zhang, V. Troung, X. F. Hu, *Appl. Phys. A* **2002**, *74*, 89.
- [32] Y. Vlasov, V. Astratov, A. Baryshev, A. Kaphyanski, O. Karmov, M. Limonov, *Phys. Rev. E* **2000**, *61*, 5784.
- [33] A. Chutinan, M. Mochizuki, M. Imada, S. Noda, *Appl. Phys. Lett.* **2001**, *79*, 2690.
- [34] M. S. Unlu, M. K. Emsley, O. I. Dosunmu, *J. Vac. Sci. Technol. A* **2004**, *22*, 781.
- [35] R. V. Kruzelecky, S. Zukotynski, *Mater. Sci. Forum* **1993**, *140*, 89.
- [36] R. V. Kruzelecky, S. Zukotynski, C. I. Ukah, F. Gaspari, J. M. Perz, *J. Vac. Sci. Technol. A* **1989**, *7*, 2632.
- [37] W. Stöber, A. Fink, E. Bohn, *J. Colloid Interface Sci.* **1968**, *26*, 62.
- [38] H. Giesche, *J. Eur. Ceram. Soc.* **1994**, *14*, 205.